CHAPTER 3

EXPERIMENTAL METHOD

3.1 Introduction

The experimental part of this work starts with thin films preparation and device fabrication. Chapter 3 describes the substrate preparation, thin film and device fabrication. The solution processing method of spin coating and thermal evaporation technique that have been used in this work are explained in details. Consequently, the characterization setup for both thin film and device are described. The characterization techniques used for the thin film are Fourier transform Infrared (FTIR), X-Ray diffraction (XRD), optical absorption and photoluminescence (PL) spectroscopy, thickness measurements and atomic force microscopy (AFM). While the characterizations techniques used for the OLED device involves are current-voltage-luminance (I-V-L) measurement and impedance spectroscopy.

3.2 Substrates and Their Preparation

Glass, Silicon (Si) wafer and Indium Tin Oxide (ITO) were used as substrates for the fabrication thin film and OLED devices. Each substrate has identical physical properties for different experimental applications. Glass is transparent, so it is suitable for UV-VIS absorption spectroscopy of thin film. Photoluminescence measurement also can be performed to the thin film deposited on a clean glass substrate. On the other hand, Si substrate is suitable for Fourier Transform Infra Red (FTIR) measurement because the IR ray can be transmitted though the substrate [*Zhu, 2004*]. An ITO-coated glass substrate is a transparent metal thin film that is used as an anode in OLED fabrication due to its high work function [*Guang-Feng et al., 2007*]. High work function means that a hole can be easily injected out from the ITO surface to enter the organic thin film when a sufficient voltage (to overcome the barrier height potential) is applied to the device as been explained in Chapter 2. The barrier height potential is however, depends on the high occupied molecular orbital (HOMO) level of those particular organic materials.

Substrate preparation process is an important procedure which can be used to control experimental parameter, such as the size of an active area of an OLED. Appropriate substrate preparation process can be used to avoid contamination in the thin films and devices. The process includes cutting and cleaning, and also etching of an ITO substrate. Initially, the substrates were cut on to a size of 2.2 cm × 2.3 cm using a diamond cutter. The substrates were then cleaned using a specific method for a different type of substrates.

The glasses were cleaned through the cleaning procedure as described below:

1) The substrates were put in a beaker containing soap water. The whole beaker was immersed into an ultrasonic bath for 15 minutes to remove contamination coming from dust and small particle.
2) The substrates were then rinsed with distilled water to remove the remaining soap water from their surfaces.
3) The substrates were rinsed with acetone to remove non-polar type contamination.
4) The substrates were quickly rinsed with ethanol in order to remove polar type contamination.

5) The substrates were rinsed with deionized water to remove ethanol solvent.
6) The cleaned substrates were purged with nitrogen gas for drying proposes.

The Si substrates were cleaned using the following steps:

1) The substrates were initially rinsed with deionized water.
2) The substrate were immersed into a solution of H_2O_2:HCL with the ratio of 1:1.
3) The substrates were then immersed into a solution of NaOH with the ratio of 1:1.
4) The substrates were immersed into a solution of HF:H_2O with ratio of 1:9.
5) The substrates were rinsed with deionized water before they were purged with nitrogen to dry.

For ITO substrates, the cleaning procedure was almost the same as that of glass. The different was only for the step no. (4), instead by using ethanol, iso-propanol was used to avoid destruction in the surface morphology of the substrate.

Prior to the cleaning process, the ITO substrates have to be patterned in order to avoid short circuit due to the metal cathode diffusion during any electrical measurement. For this purpose, the ITO substrates have to go through the wet etching process which was carried out as follows:

1) The ITO substrates were cut into the size of 2.1 cm × 2.3 cm.
2) 2/3 of the ITO surface were covered with a commercialize spray paint.
3) The ITO substrates were boiled in a diluted hydrochloric acid (HCl:H_2O=9:1) at the constant temperature of 120^oC for 15 minutes to etch the 1/3 uncovered part of ITO surface.

4) After the ITO substrates were cooled down to room temperature, the part which was covered by paint was ultrasonically removed by immersing the ITO into an acetone solvent.
5) Finally, the patterned ITO substrates were cleaned again by going through the cleaning procedure as described previously. The typical patterned ITO substrate is shown in Fig. 3.1.

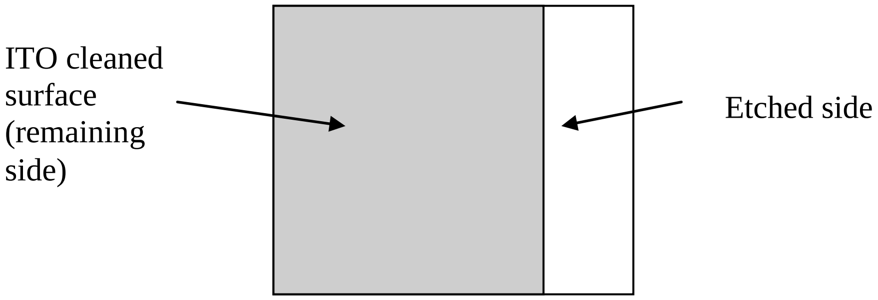

Figure 3.1: Diagram of patterned ITO

3.3 Solution Preparation

Organic solutions in this study were prepared by dissolving the materials in the form of powder into chloroform solvent ($CHCl_3$) with respective dopant systems. The concentration of the solutions was fixed at 10 mg/mL in order to get approximately the same film thickness for the same spin rate. The solutions were prepared in a clean room environment at atmospheric pressure which is also called as the air-processed fabrication condition.

The main materials in this study are; tris(8-hydroxyquinoline)aluminium (Alq_3), *N,N'*-diphenyl-*N,N'*-bis(3-methylphenyl)-1,1'-biphenyl-4,4'-diamine (TPD), and 2-(4-biphenylyl)-5-phenyl-1,3,4-oxadiazole (PBD). They were purchased from Sigma Aldrich and were used without further purification. The materials were initially weighed by using a digital weighing system. The weight and calculation of the concentration for different dopant system are listed in Table 3.1 below:

Table 3.1: Summary of solution preparation parameter.

System	Material	Weight (mg)	Volume of $CHCl_3$ (ml)
Single material	Alq_3 TPD PBD	20 20 20	2
TPD:Alq_3	TPD Alq_3	10 10	2
TPD:PBD:Alq_3	Alq_3 TPD PBD	10 10 10	3

After dissolving the materials, the solution was stirred by using a magnetic stirrer bar at 500 rpm in 10 minutes in order to ensure that the materials were well dissolved in $CHCl_3$ solution.

3.4 Thin Film and OLED Fabrication

The thin films and OLED devices in this study were prepared by using a spin coating technique. The spin coater model Laurell WS-400B-6NPP/LITE was used and the image is shown in Fig. 3.2. High pressure air is needed to make the motor system operated. Thus, this apparatus was connected to the air compressor by a plastic host. A rotary pump was connected to the bottom of the platform where a substrate is placed on the top of it. This vacuum system was set to hold the substrate and avoid them from spreading away while coating process was performed. The system itself has been developed with a safety system where the instrument cannot be operated if air and vacuum pressure was not sufficient.

The spinning parameters were initially setup for a desired film thickness. The spin speed and duration were set to be 2000 rpm and 40 second, respectively in order to get an approximately 80 to 85 nm film thickness for a solution prepared at 10 mg/mL concentration. The thin film fabrication process is described in the flow diagram in Fig. 3.3. Fig. 3.4. describes the fabrication process of an OLED device investigated in this work.

Figure 3.2: Laurell WS-400B-6NPP/LITE spin coater system

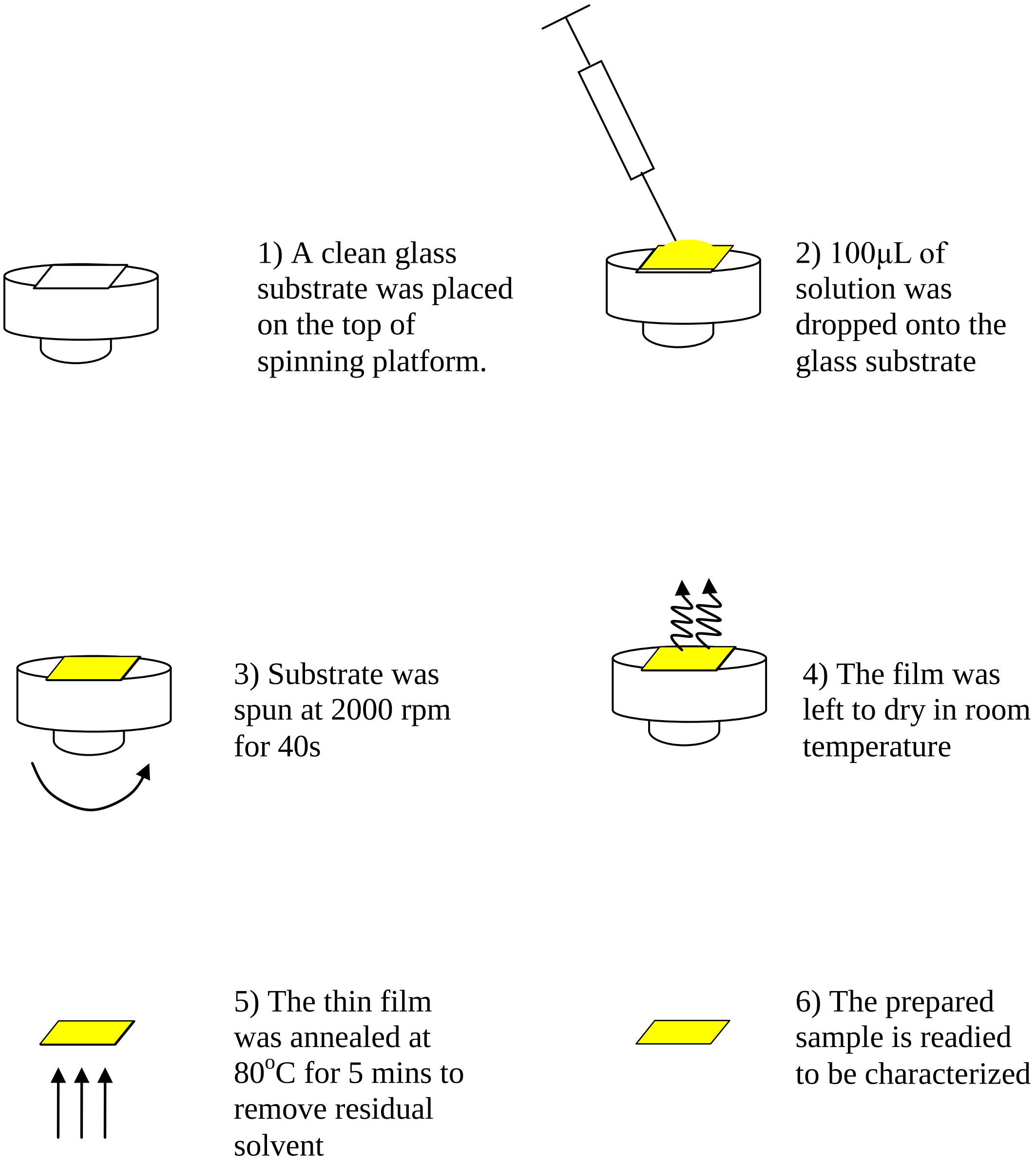

Figure 3.3: Fabrication process of a thin film using the spin coating technique

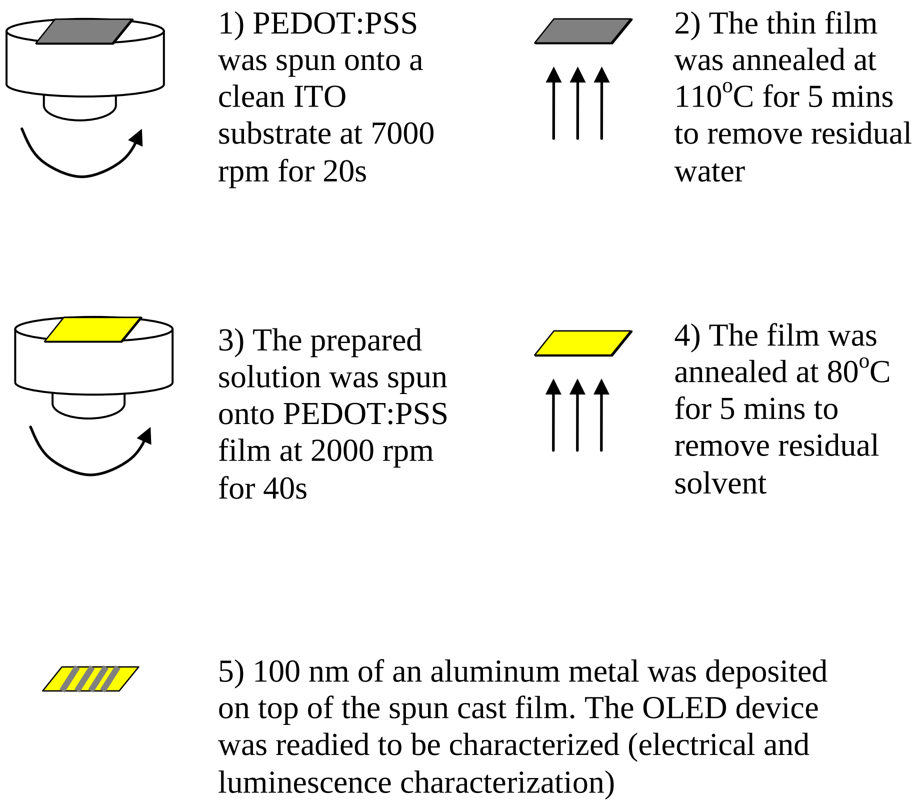

1) PEDOT:PSS was spun onto a clean ITO substrate at 7000 rpm for 20s

2) The thin film was annealed at 110°C for 5 mins to remove residual water

3) The prepared solution was spun onto PEDOT:PSS film at 2000 rpm for 40s

4) The film was annealed at 80°C for 5 mins to remove residual solvent

5) 100 nm of an aluminum metal was deposited on top of the spun cast film. The OLED device was readied to be characterized (electrical and luminescence characterization)

Figure 3.4: The fabrication process of an OLED

It is noted that the solution of PEDOT:PSS was spun coated, initially on top of the ITO layer at 7000 rpm for 20 s to form a buffer layer with thickness of 20 nm. An ultra thin layer of PEDOT:PSS is commonly used to refine surface roughness of the ITO substrate that is usually high after cleaning process [*Kim et al., 1998; Wantz et al., 2005*]. The thin layer of PEDOT:PSS is also acting as a hole injection layer (HIL) as its HOMO level is higher than the electron affinity of the ITO substrate [*Petr et al., 2004*]. Aluminum (Al) was used as the metal cathode in this work due to their low work function compared to that of ITO [*Lee et al., 2006; Lü et al., 2011*]. After the organic layer has been spin coated on the top of ITO/PEDOT:PSS layer, a top Al electrode was deposited using the thermal evaporation technique. The thermal evaporator system that has been used was Auto Edward 306 deposition system. A typical diagram of the thermal evaporator system is shown in Fig. 3.5. Al deposition process was done in the vacuum environment of 2.5×10^{-5} mbar. Several pieces of Al source (wire) were attached on a coil of tungsten filament that acts as a heating source. A current 17 to 25 A was used to heat up the tungsten filament until the Al wires melted and started to vaporize. A shuttle was opened to let the melt Al evaporated upwards to the samples and at the same time, a thickness monitor was on to count the evaporation rates and thickness of the deposited Al. The evaporation rate was maintained around 2 nm/s to avoid Al particles from diffusing into the organic layer. After a desired thickness was achieved, the shuttle was closed and the current was reduced slowly until a zero reading was obtained. Fig. 3.6 shows a typical structure of the OLED device fabricated in this works.

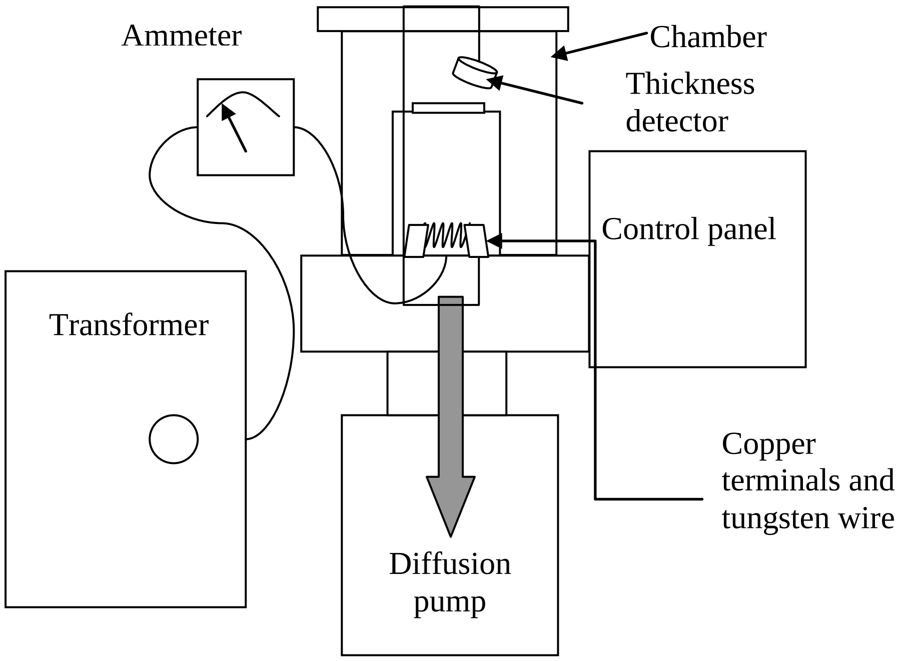

Figure 3.5: Typical thermal evaporation deposition system

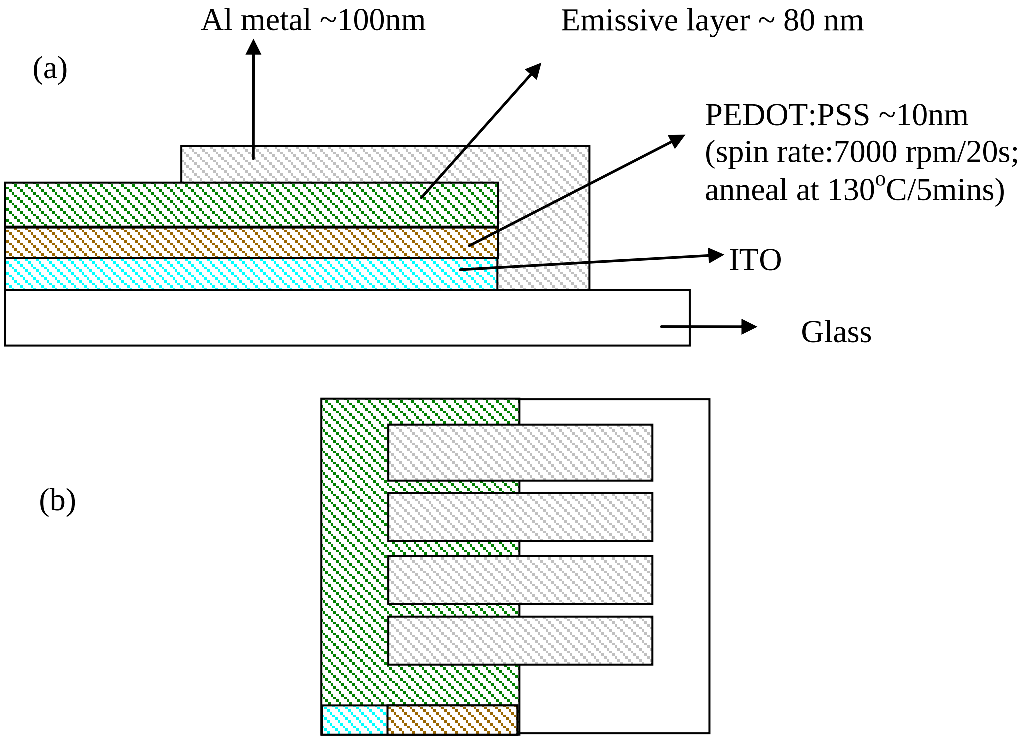

Figure 3.6: A typical construction of an OLED device fabricated in this work. (a) a side view and (b) a top view of the fabricated OLED device.

3.5 Fourier transform Infra red (FTIR) Spectroscopy

Molecular vibrations of the thin films were obtained from Perkin Elmer System 2000 FTIR spectrometer. FTIR spectrometer is a useful instrument to extract information on the structure of the materials. The interaction of the infrared radiation makes two atoms bonded together to vibrate as if connected by a spring-like bond. The operation of the spectrometer starts with a beam of infrared source generated and passed through a Michelson interferometer. The beam is then incidents on the sample (thin film) where some of the ray is absorbed by a particular vibration mode of the sample. The beam finally enters a detector and the light signal is translated to an electrical signal so that it can be interpreted by a computer as an IR interferogram spectrum. The optical pathway of the system is shown in Fig. 3.7.

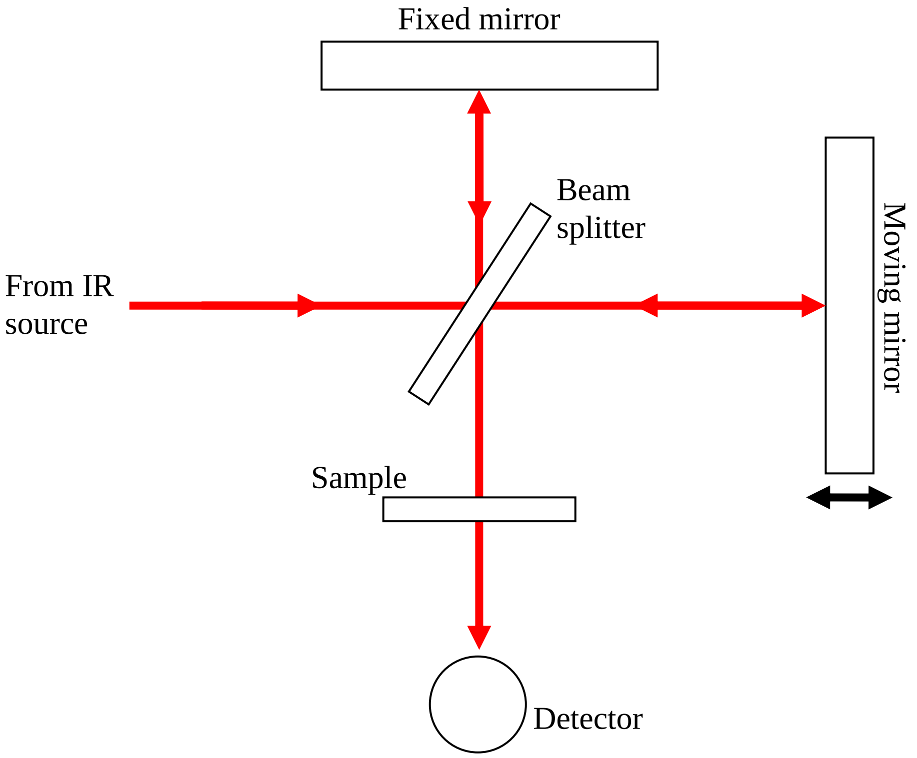

Figure 3.7: Schematic diagram of optical path in FTIR measurement

The FTIR spectrum of a sample is obtained after subtracting it with the spectrum of the substrate which is scanned prior to scanning sample. Table 3.2 shows the measurement parameters of the FTIR spectroscopy used in this work.

Table 3.2: Parameter of the FTIR measurement

Range	3000 cm^{-1} to 400 cm^{-1}
Number of scan	10
Resolution	5.0 cm^{-1}
Unit	Transmission

3.6 X-Ray Diffraction (XRD) Spectroscopy

The XRD measurement was performed by Siemens D5000 (XRD) Instrument. The instrument is based on crystallography which is related to the X-rays diffraction pattern which is produced by atoms at a lattice point of material. Inter planar distance of atoms in the materials can be determined by using Bragg's law [*Konry & Marks*, *2005*]. However, for amorphous sample, the XRD pattern is broad and no significant peak can be observed due to an irregular structure of the atom inside the material. The sample in the form of thin film was placed on sample platform. Table 3.3 shows the parameters used for the XRD measurement.

Table 3.3: Setup of XRD measurement

Fixed div slit	1.0 nm
Fixed sample slit	1.0 nm
Fixed detector slit	0.1 nm
Anode	Copper
Mode	2-theta

Step time	2 second
Step size	0.05^{o}
Start	5.00^{o}
End	80^{o}

3.7 UV-Vis-NIR Spectroscopy

In this work, UV-VIR-NIR Jasco model V-570 was used to analyze the optical properties of the prepared organic thin films. The light path of UV-Vis-NIR spectrometer is shown in Fig. 3.8. This equipment can be used to measure the spectrum at a wavelength range from 250 to 2500 nm. A deuterium discharge tube (wavelength range 190nm to 350 nm) and a tungsten iodine lamp (wavelength range 340nm to 2500nm) were used as a light source in the UV region and visible to near infrared region, respectively.

The beam light was covered before entering the monochromator. It was spread by a grating in the monochromator and the light was passed through the exit slit of the monochromator. This light was split into two light paths by a sector mirror, one incident on the sample to be measured and the other one on the reference sample. The light that has passed through the sample or reference sample was then incident on the photomultiplier tube or plumbum sulfide (PbS) photoconductive cell.

The light from PbS photoconductive cell was converted into an electrical signal which was then decoded into a digital form. The signal was processed and executed by software which will then display as a spectrum for the film. Light source change and wavelength trigger during the measurement process are controlled by operation software.

Upon starting the measurement, two cleaned glass substrate (references) were placed in the sample holder for scanning in order to produce the baseline for the absorption spectrum in the wavelength range of 200 nm to 800 nm. This scanning range was selected due to the strong absorption of organic semiconductor materials between UV and visible region. Then, one of the glass substrate was removed and replaced with the organic thin film deposited on glass, while the other remained to acts as a reference. The absorption spectrum of the sample was obtained within the same wavelength range of 200 nm to 900 nm.

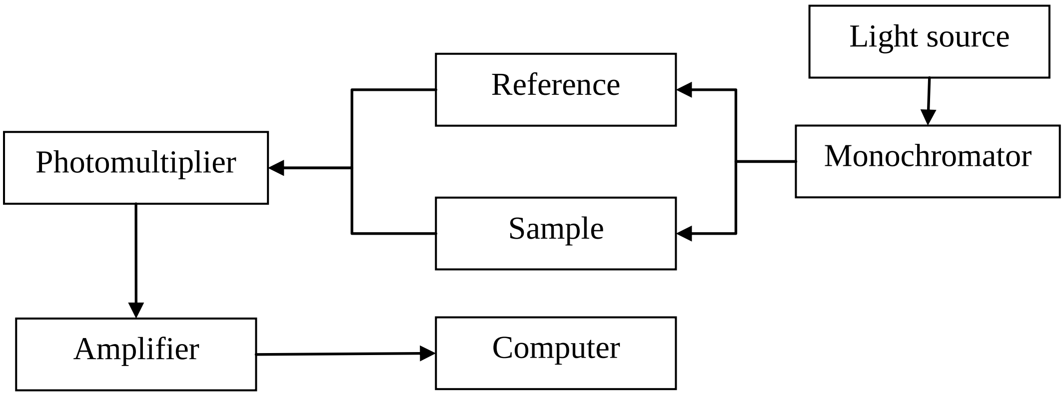

Figure 3.8: Light path of the spectrometer UV-Vis-NIR

From the absorption spectrum, the optical energy gap can be obtained. The optical energy gap is the energy different between the high occupied molecular orbital (HOMO) and lowest unoccupied molecular orbital (LUMO). In the other words, it represents the minimum energy for excitation of electron between these two energy levels. The optical energy gap, E_g is calculated from the Tauc relation [*Muhammad et al., 2010*].

$$\alpha hv = B(hv - E_g)^n \qquad (1)$$

where α and B are the absorption coefficient and Tauc coefficient, respectively. h and v are the Planck constant and velocity of light, respectively. The n is equal to ½ for a direct band semiconductor and E_g is the energy band gap of the semiconductor. The absorption coefficient is obtained from the ratio of the absorption spectrum over the thickness of the thin film, as shown by:

$$\alpha = 2.203\frac{A}{d} \tag{2}$$

where A is absorbance spectrum and d is the thickness of film. Eq. (2) is differentiated with respect to photon energy, hv, and by converting it to natural logarithm, the determination of n value, can be simplified as:

$$\frac{\partial \ln(\alpha hv)}{\partial hv} = \frac{n}{hv - E_g} \tag{3}$$

An extrapolation plot of $(\alpha hv)^2$ versus photon energy, hv gives the value of the optical band gap of the thin film. Since, $E_g=hv$ when $(\alpha hv)^2=0$, then the E_g can be refer as the interception at x-axis when the value A=0.

3.8 Photoluminescence Spectroscopy

The photoluminescence (PL) spectroscopy measurement of organic thin films was performed by Perkin Elmer LS 50B Luminescence Spectrometer. The spectrometer consists of an optical path as shown in Fig. 3.19. A light source for the excitation was a gas discharge lamp of Xenon with high pressure that gives near ultraviolet (UV) and visible emission spectrum. This lamp can emit a continuum spectrum from 200 nm up to 700 nm of wavelength. A grating monochromator was used to disperse the excitation light into its component of wavelength. A control slit was set to select the band of the incident light coming from the monochromator. The excitation light then entered the filter and polarizer wheel for stabilizing the light polarity. A small reference photomultiplier detecting a noise so that the PL spectrum that comes out was stable. The excitation light was then excited the thin film located in the sample holder. After the sample has been excited with a selected wavelength, the photoluminescence emission went into polarization and grating process, and then finally entered the sample photomultiplier.

The specific software of FL WinLab is used to control all the experimental setup. By using this software, a user is allowed to select the excitation wavelength, excitation and emission slit width and the desired scan speed. Spectrum data can be viewed and analyzed just after the sample has been scanned. The scanning parameter that has been used in this work is tabulated in Table 3.4.

Table 3.4: Scanning parameter for PL measurement

Scan menu	Emission
Excitation wavelength	Depends on the highest absorption of the sample determined from UV-Vis-NIR result
Excitation slit	10 nm
Emission slit	10 nm
Scan speed	800 min/ nm

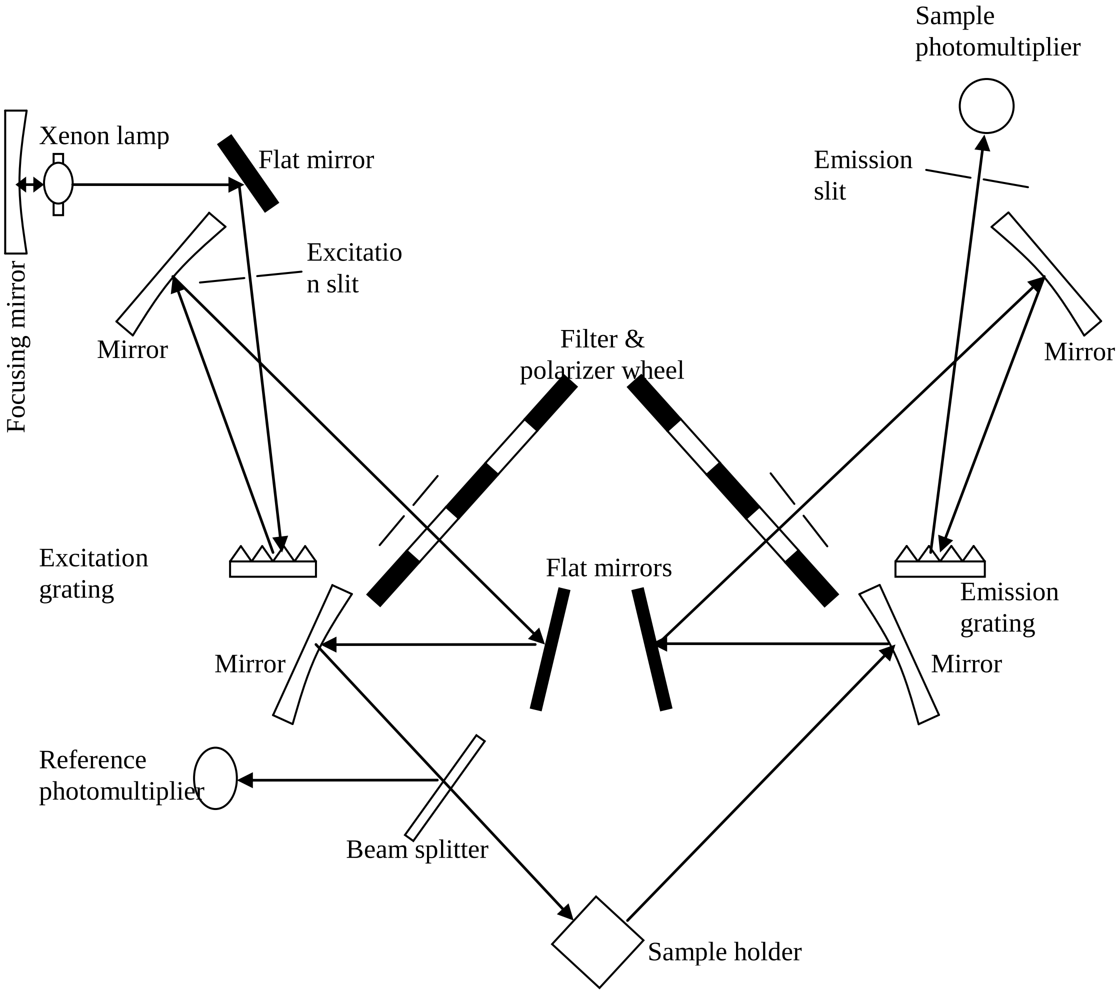

Figure 3.9: Optical path of photoluminescence spectrometer

3.9 Thickness measurement

The KLA Tencor P-6 profilometer was used to determine the thickness of the prepared organic thin films for this study. The P-6 profiler analysis system is a powerful apparatus for surface topography analysis. Additionally it is smaller and more economical design for substrates up to 150 mm in size. The thickness of the thin film was measured from the steps height different between the substrate (base) and the thin film layer. Fig. 3.10 shows a typical measurement for determining thickness of a thin film. The thin film was carefully scratched to form the different height.

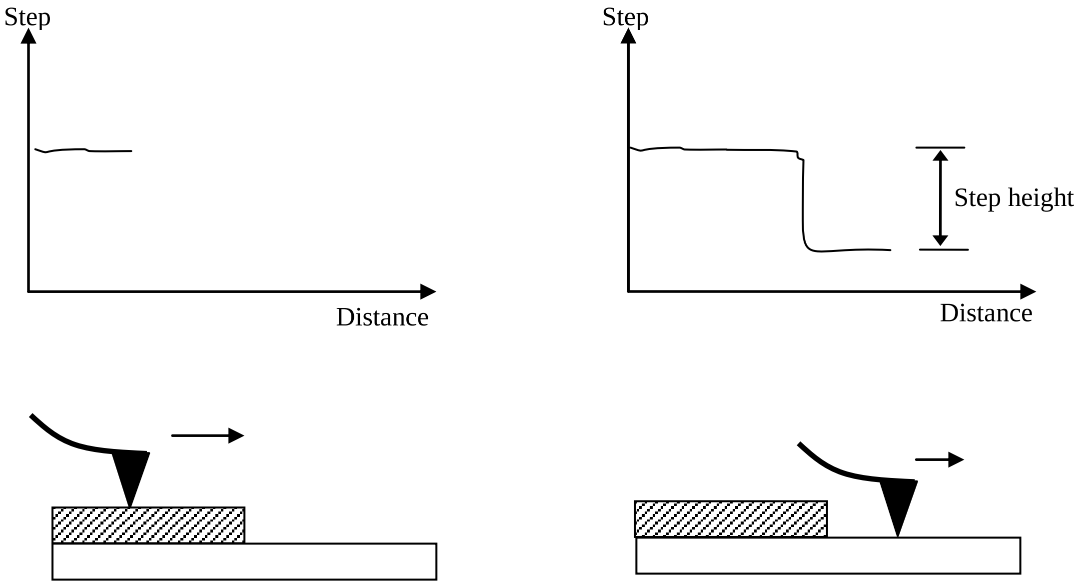

Figure 3.10: A typical measurement of thickness using the step height difference method. Stylus tip is moving in the given direction and the surface profile of the sample is shown in the graph. The thickness is determined from the step height. The white and shaded rectangular represents the substrate and the thin film layer, respectively.

3.10 Atomic Force Microscopic (AFM)

The Veeco P3000/NS3A-digital instrument was used in the atomic force microscopy measurement in this work. The AFM probe was mounted into the cantilever holder. Then, the cantilever holder was loaded to the APM. The laser was set to be aligned to the tip. Then, the photo detector was adjusted to the significant alignment to detect the laser that comes in. The cantilever was tuned and the initial scan parameter was setup. The scan parameter was adjusted to the suitable condition to get a good AFM image. The scan size, scan rate, image data was 5µm, 2.00 Hz and height, respectively. The AFM image was then captured and saved. The AFM image was analyzed to study the surface morphology of the organic thin films fabricated to be used in the OLED investigated.

3.11 OLED Characterization

The current-voltage-luminance (*J*-*V*-*L*) characteristics of the devices were measured using a Konica Minolta CS-200 chromameter (refer Fig. 3.11 (a)) and a Keithley 2400 source measure unit (SMU). The setup of the J-V-L measurement is illustrated in Fig. 3.11 (b). CS-200 chromameter is a high-precision measurement for luminance and chromaticity comparable to spectroradiometers. The instrument is a tristimulus type where the measurement of light sources is performed by three sensors of red, green and blue. This high sensitive sensor is similar to sensitivity of human eye towards light. Even the sensors are highly sensitive, the precision of reading still limited by the filters used and most accurate reading can be achieved if the distribution of spectra are similar to that of the light source used for calibration. In order to overcome this problem, the measured spectral of the light will be calculated mathematically using the spectral sensitivity characteristics where the colour matching function is used. This calculation is corresponds to the sensitivity of human eye, thus the measurement result become more precise. The CS-200 can measure from 0.01 cd/m^2 to 20,000,000 cd/m^2, which give an advantage for wide range of light measurement. S-S10w Standard Edition was used as an interface to control the CS-200 via a computer where the list of measured data was displayed or transferred to spreadsheet software. The common features of CS-S10w include instrument control, data management and data evaluation.

The Keithley 2400 SMU was used to apply the driven voltage to the OLED device and also measured the respective current from it. The driven voltage was varied from 0 to 15V with an interval of 0.5V. The duration for each point of measurement was set to be 0.1s to avoid Joule heating that might damage the device. Every device consisted of four pixels which represent four devices in one fabrication (as shown in Fig. 3.12). Thus the measurement system was equipped with a device holder that has four sensitive tip-contacts which acted as the contact for negative terminal and another one tip for the positive terminal. These tips were fabricated with a small spring attached to its end in order to minimize the force between the tip and the pixels of the device to avoid damage to the device. The devices were placed in a built-in dark-box opposite the CS-200 lens to avoid the effect of the surrounding light to the measurement reading. All the measurements were done in room environment without encapsulation.

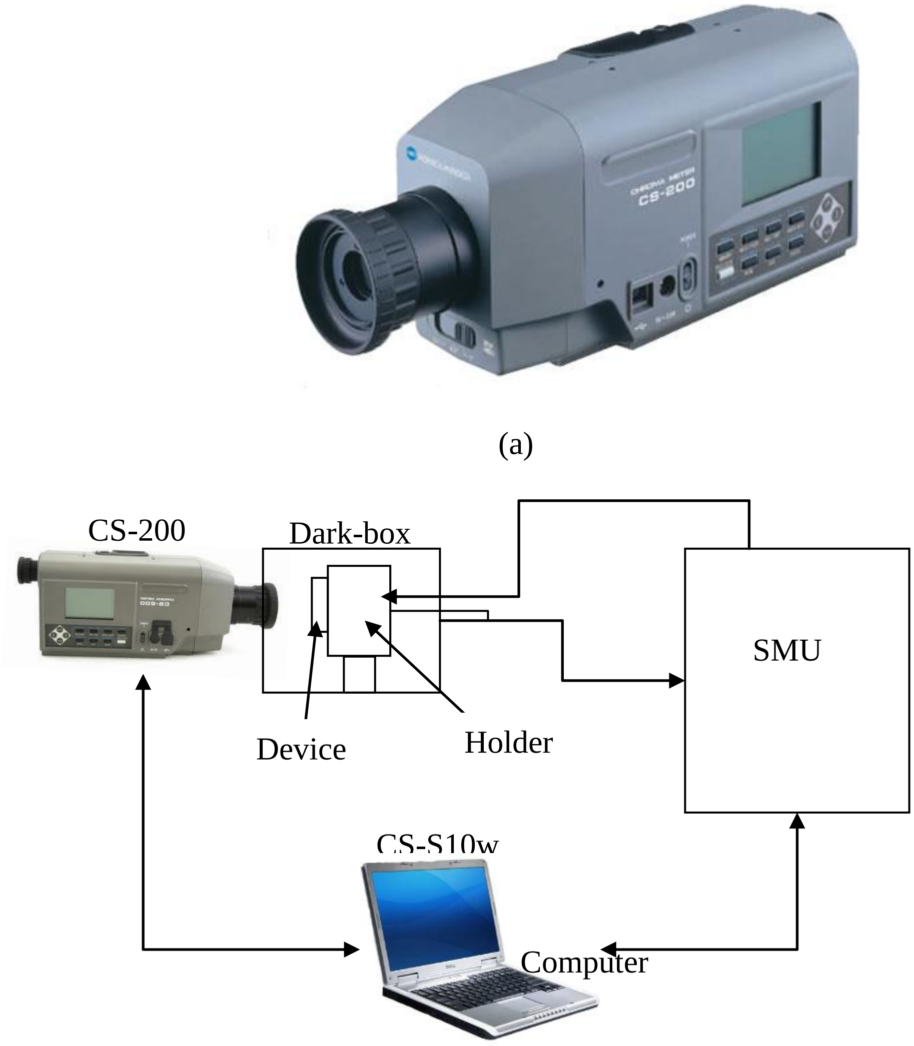

(a)

(b)

Figure 3.11: (a) Konica Minolta CS-200 and (b) experimental setup for electrical and luminescence characterization of the device

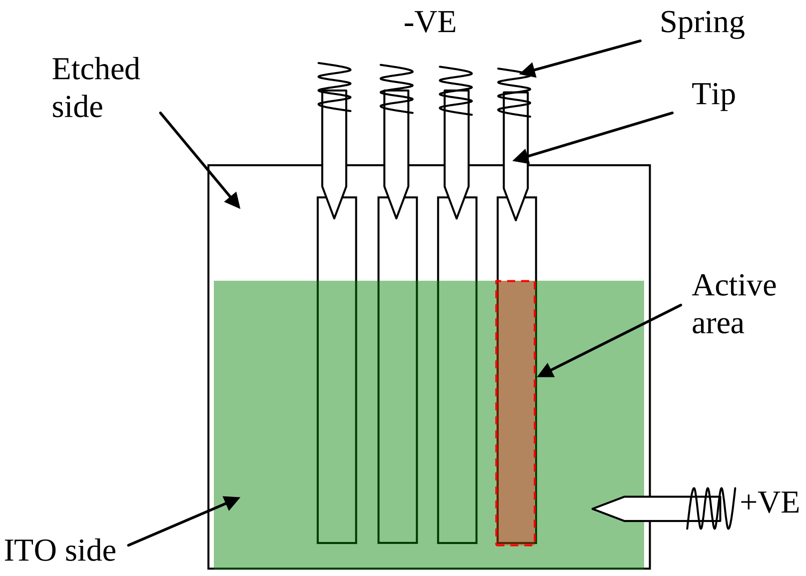

Figure 3.12: A schematic diagram of the device holder. It consists of tips with spring at end of it. The shaded part is the ITO side and the non-shaded part is the etched part. The active area of the device marked as the red box, where the ITO, the organic film and the metal cathode are coincided with each other.

From the device characterization, the current-voltage (*I*-*V*) and luminance-voltage (L-V) data were obtained. In order to change the unit of current to current density, *J*, the current value obtained is divided with the size of an active area of the device,

$$\text{current density, } J = \frac{I}{A}$$

where *I* the is current in Ampere and *A* is an active area in meter. Then, according to the formula of power efficiency,

$$\eta = \frac{\pi L}{VJ} = \pi \frac{1}{V}\left(\frac{L}{J}\right) = \pi \frac{\gamma}{V}$$

where η is the power efficiency and γ is the current efficiency of the device. In this work, the device efficiency only refers to the point where the highest luminance is achieved.

3.12 Impedance Spectroscopy

Impedance characterization was performed by using a 1260 Impedance/gain-phase Analyzer (Solatron) from Pusat Asasi Sains Universiti Malaya. The equipment was setup to measure parallel circuit of the OLED device. 1296 dielectric interface was used as a connector between the equipment and the OLED device. The OLED devices were measured within the frequency range from 10^{-1} to 10^{5} Hz and the amplitude of the AC bias was 20 mV which is relatively much lower compared to that stated in ref. [*Ishihara et al., 2011*]. However, there is also a report of a group that has as low as 10 mV of the AC bias to measure impedance of MEH-PPV based OLED [*Rouis et al., 2007*].

3.13 Summary

Thin films and OLED devices were prepared using spin coating technique in ambient air environment to optimize the simple and robust fabrication method. The characterizations of the thin films were performed to study the optical, structural and morphology of the organic materials in solid state form. The characterizations of the OLED devices were performed to analyze the light output and dielectric properties of the devices.

References

Guang-Feng, W., Xiao-Ming, T., & Rong-Xin, W. (2007). Highly Conductive Flexible Transparent Polymeric Anode and its Application in OLEDs. Paper presented at the Electronic Components and Technology Conference, 2007. ECTC '07. Proceedings. 57th.

Ishihara, S., Hase, H., Okachi, T., & Naito, H. (2011). Determination of Charge Carrier Mobility in Tris(8-hydroxy-quinolinato) Aluminum by Means of Impedance Spectroscopy Measurements. Organic Electronics, 12, 1364-1369.

Kim, J. S., Granstrom, M., Friend, R. H., Johansson, N., Salaneck, W. R., Daik, R., et al. (1998). Indium--Tin Oxide Treatments for Single- and Double-Layer Polymeric Light-Emitting Diodes: The Relation Between the Anode Physical, Chemical, and Morphological Properties and the Device Performance. Journal of Applied Physics, 84, 6859-6870.

Konry, T., & Marks, R. S. (2005). Physico-Chemical Studies of Indium Tin Oxide-Coated Fiber Optic Biosensors. Thin Solid Films, 492, 313-321.

Lee, J.-H., Jeong, J.-H., Suh, C.-H., Kim, Y. K., Park, N. G., & Kim, Y. S. (2006). Numerical Analysis of OLED Using the Hetero Electrode. Current Applied Physics, 6, 654-657.

Lü, Z., Deng, Z., Chen, Z., Yin, Y., Xu, D., Xiao, J., et al. (2011). The Effect of Various Electrodes on the Properties of Electroluminescent Devices with Potassium Chloride Inside Tris (8-Hydroxyquinoline) Aluminum. Displays, 32, 113-117.

Muhammad, F. F., Abdul Hapip, A. I., & Sulaiman, K. (2010). Study of Optoelectronic Energy Bands and Molecular Energy Levels of Tris (8-Hydroxyquinolinate) Gallium and Aluminum Organometallic Materials from Their Spectroscopic and Electrochemical Analysis. Journal of Organometallic Chemistry, 695, 2526-2531.

Petr, A., Zhang, F., Peisert, H., Knupfer, M., & Dunsch, L. (2004). Electrochemical Adjustment of the Work Function of a Conducting Polymer. Chemical Physics Letters, 385, 140-143.

Rouis, A., Mlika, R., Davenas, J., Ben Ouada, H., Bonnamour, I., & Jaffrezic, N. (2007). Impedance Spectroscopic Investigations of ITO Modified by New Azo-Calix[4]Arene Immobilised into Electroconducting Polymer (MEHPPV). Journal of Electroanalytical Chemistry, 601, 29-38.

Wantz, G., Hirsch, L., Huby, N., Vignau, L., Silvain, J. F., Barriére, A. S., et al. (2005). Correlation Between the Indium Tin Oxide Morphology and the Performances of Polymer Light-Emitting Diodes. Thin Solid Films, 485, 247-251.

Zhu, J. (2004). Backside Analysis Using Re-Package Techniques. *Microelectronics Failure Analysis: Desk Reference Fifth Edition* (5th ed., pp. 341-346). Texas: ASM International.